separations

MDPI

Article

Biosorption of Manganese Using *Moringa oleifera* Seed Pods: A Sustainable Approach to Water Treatment

Laura Adriane de Moraes Pinto [1], Fernanda de Oliveira Tavares [2], Rosangela Bergamasco [2], Marcelo Fernandes Vieira [2] and Angélica Marquetotti Salcedo Vieira [1,*]

[1] Postgraduate Program in Food Science, Universidade Estadual de Maringá, Maringá 87020900, PR, Brazil; lauraampinto@gmail.com

[2] Postgraduate Program in Chemical Engineering, Universidade Estadual de Maringá, Maringá 87020900, PR, Brazil; fernanda_tavares_15@hotmail.com (F.d.O.T.); rbergamasco@uem.br (R.B.); mfvieira2@uem.br (M.F.V.)

* Correspondence: amsvieira@uem.br; Tel.: +55-44-3011-5093

Abstract

Manganese (Mn) has emerged as a contaminant of concern due to its occurrence at concentrations exceeding regulatory limits in various environmental matrices, driven by both anthropogenic activities and natural geochemical processes. Although Mn is an essential micronutrient, excessive exposure poses risks to human health and ecosystems. This study investigates the potential application of *Moringa oleifera* seed pods, an agro-industrial byproduct, as low-cost biosorbents for Mn ion removal from aqueous solutions. Biosorbents were prepared from raw seed pods and chemically modified using NaOH and HCl. Surface characterization was performed using SEM, EDS, and FTIR techniques. Kinetic analysis indicated that Mn ion adsorption by all biosorbents followed a pseudo-second-order model, with equilibrium reached within 30 min. Among the tested materials, the alkali-treated biosorbent exhibited the highest removal efficiency (94%) under optimal conditions (288 K, pH 6.0, 60 min). Equilibrium data fitted both Langmuir and the Freundlich isotherms, with a maximum adsorption capacity of 7.64 mg g^{-1} for alkali-treated pods and 6.00 mg g^{-1} for the unmodified pods. Thermodynamic analysis revealed negative Gibbs free energy values, confirming the spontaneous nature of the biosorption process. Enthalpy values below 40 kJ mol^{-1} (Pod_{NA}: 11.88 kJ mol^{-1}; Pod_{AC}: 1.08 kJ mol^{-1}; Pod_{BA}: 8.94 kJ mol^{-1}) suggest that physisorption is the predominant mechanism. These findings demonstrate the viability of *Moringa oleifera* pods as effective biosorbents for Mn ion remediation, supporting the valorization of agricultural waste within sustainable water treatment strategies.

Keywords: emerging contaminants; heavy metals; sustainability; waste utilization; biosorption; bresh pod shell; chemical modification; oilseed

check for updates

Academic Editors: Xin Zhou, Shouqing Ni and Guoqiang Liu

Received: 28 June 2025
Revised: 2 September 2025
Accepted: 3 September 2025
Published: 9 September 2025

Citation: de Moraes Pinto, L.A.; de Oliveira Tavares, F.; Bergamasco, R.; Vieira, M.F.; Vieira, A.M.S. Biosorption of Manganese Using *Moringa oleifera* Seed Pods: A Sustainable Approach to Water Treatment. *Separations* **2025**, *12*, 246. https://doi.org/10.3390/separations12090246

Copyright: © 2025 by the authors. Licensee MDPI, Basel, Switzerland. This article is an open access article distributed under the terms and conditions of the Creative Commons Attribution (CC BY) license (https://creativecommons.org/licenses/by/4.0/).

1. Introduction

The contamination of aquatic environments represents a critical global concern, contributing substantially to the incidence of various diseases and elevated mortality rates worldwide. Heavy metals, such as manganese (Mn), are frequently detected in industrial effluents, primarily originating from mining, metallurgical processes, and manufacturing activities [1].

Manganese is naturally present in groundwater and, even at low concentrations, can cause several problems in water quality, making its removal essential [2]. Consumption of food and water contaminated with heavy metals is a significant route of human exposure

to metals, accounting for approximately 90% of cases. In this regard, the risks associated with metal contamination in foodstuffs have aroused considerable concern worldwide [3]. Although manganese (Mn) and certain micronutrients are essential for plant growth and human nutrition, they become toxic to the body in high concentrations, as they are not biodegradable and can cause serious adverse effects on human health [4].

Manganese (Mn) is essential for neuronal health but neurotoxic in excess [5]. It is responsible for some diseases, such as Parkinson's disease, and causes damage to the brain, liver, kidneys, and nervous system; in pregnant women, it affects fetal development and induces abortion, as well as being neurotoxic for children [6,7].

The presence of manganese in water is a concern for both the population and industry. High-quality water is of great importance for producing safe foodstuffs. In the food industry, water is used in all operations, whether directly incorporated into the product as an ingredient or a vehicle for combining ingredients into formulations, or indirectly in processes such as fluid for heat transfer, cleaning and sanitizing equipment, and areas of the process [8]. The presence of manganese in water is directly linked to the oxidation and corrosion of pipes, and it is primarily responsible for imparting an odor, metallic taste, and black discoloration to water distribution and supply systems [9]. Fouling and corrosion in pipes, equipment, and cooling systems increase maintenance costs, reduce operational efficiency, and are a significant source of contamination by manganese [10].

The US Environmental Protection Agency (EPA) [7] sets a maximum level of manganese in drinking water of 0.05 mg L^{-1}. Similarly, the World Health Organization (WHO) [11] has established a limit of 0.1 mg L^{-1}. This limit is the same as adopted in Brazil; the resolution of the National Environment Council (CONAMA) number 357/2005 [12] allows 0.1 mg m^3 for total manganese to freshwater class I and II.

There is clear evidence of elevated manganese levels in surface waters and effluents, as presented in several works [13–16]. Therefore, this type of contamination is observed in the most diverse locations around the world, being found in both regions of Brazil, including rivers and industrial effluents, as well as in areas impacted by mining in the Philippines and China.

The survey of metal levels in rivers in the industrial town of Sasolburg revealed higher mean concentrations of Mn, exceeding the guideline limits for domestic and agricultural use set by the WHO and EPA (>50 μg L^{-1}) [15]. High levels of Mn, among other metals, which exceed the maximum permissible concentration limit set by international regulatory organizations, were found by Agarin et al. [17] in waters off an island in the Philippines.

The study carried out by Hermes et al. [13], taking water samples from the surface of the Pardinho River, RS, Brazil, identified that the mean results of total Mn were in the order of 113.3 μg L^{-1}. A water quality assessment carried out by Melo et al. [14] on waters from the Una-Pernambuco River Basin found Mn levels of 0.53 mg L^{-1}. The authors also mention that around 80% of the samples from the Panelas River showed concentrations of this metal above the legal limit, 0.1 mg L^{-1}, established by WHO.

Other references mention high levels of Mn in groundwater, such as 0.38 mg L^{-1} in Jashor, Bangladesh, 1.9 mg L^{-1} in Lampang, Thailand [18], and 6.16 mg L^{-1} in Shuangliao, China [19]. Therefore, it is understood that the effective removal of these contaminants from wastewater is crucial for protecting environmental integrity and ensuring the health of ecosystems.

A variety of physicochemical methods are available for removing heavy metals from aqueous solutions. Among the various water treatment techniques are adsorption, coagulation, advanced oxidation, membrane separation, chemical precipitation, solvent extraction, reverse osmosis, filtration, and electrochemical treatment. Adsorption is preferred for removing heavy metal ions due to its ability to minimize the use of chemicals, ease of

handling, variety, and availability of different types of adsorbents, making it a technique considered "eco-friendly" [20,21].

Researchers have explored cost-effective methods and biomaterials for removing heavy metals from water. The biosorption process offers several advantages over conventional water purification methods, including the use of natural compounds instead of synthetic ones in water treatment, lower costs, reduced sludge production, and improved biodegradability. It is not aggressive to the environment, since most materials used are organic residues [22,23].

Lignocellulosic biomass, primarily composed of cellulose, hemicellulose, and lignin, has garnered attention as a low-cost and sustainable material for water treatment. Regarding dead biomass, agricultural residues are suitable alternatives for countries based on agribusiness, where these unwanted residues can be utilized and, in turn, avoid the costs associated with final disposal [24]. Its effectiveness as a biosorbent stems from the presence of functional groups on its surface, which can be enhanced through chemical modifications to improve contaminant removal efficiency [25]. Biosorbents such as the epicarp of macaúba [26], sugarcane bagasse [24], coconut shells [27], oil palm fruit bunch [28], apple bagasse biochar [29], rice husks [30], and bamboo-derived biochars [18], among others, have been studied over the years for the efficient removal of ions in aqueous solutions.

Among various plant-based biosorbents, *Moringa oleifera* (Moringa) stands out as the second most studied oilseed species for metal removal, accounting for 32.14% of reported studies [25]. The most commonly used biomass is obtained from the dehulled seed, which, due to its cellulose, hemicellulose, and lignin content, is classified as a lignocellulosic adsorbent [31,32]. Additionally, according to Meneghel et al. [33], *Moringa oleifera* offers the advantages of anchoring metals, renewability, and low cost, making its use attractive in biosorption processes.

Given the importance of the crops and considering that the processes involved in extracting their oils generate a wide variety of by-products and residues, it is necessary to develop alternatives for the use of these materials, thereby preventing them from becoming an environmental problem. According to Silva et al. [34], the yield of Moringa seed oil can reach 43%. The oil is rich in monounsaturated fatty acids, primarily oleic acid (~76%), indicating that it is an oilseed with a high-quality fatty acid source and therefore a high capacity for industrial production.

Moringa's industrialization is now a reality, found in a variety of applications, including beauty products and oil production. The adsorption of manganese onto *Moringa oleifera* seeds was studied by Carmo et al. [35]. However, studies using Moringa production waste, such as the pod shell, are scarce, justifying research into its use as a biosorbent to reduce the environmental impact of this waste. Therefore, this study aimed to use the shell of the *Moringa oleifera* seed pod, a byproduct of Moringa oil production, as a biosorbent to remove Mn from water with an excess of this ion, thus contributing to water treatment and reducing environmental liabilities.

To achieve greater Mn ion biosorption capacity from aqueous solutions, acid and base treatments were performed on the pod shell. We studied the influence of parameters such as pH, the adsorbent dose, and the adsorption contact time. Kinetic and equilibrium data, as well as thermodynamic parameters, were obtained.

2. Materials and Methods

All chemical products/reagents used in this study were of analytical grade. A Mn^{2+} solution (1000 mg L^{-1}) ($MnCl_2 \cdot 4H_2O$—Synth; analytical grade, Diadema, SP, Brazil) was prepared, and all other solutions were prepared by diluting this stock solution. A pH meter (Thermo Scientific Orion Versa Star Model, Waltham, MA, USA) was used to measure the

pH. The pH was calibrated with standard buffer solutions of pH 4.0, 7.0, and 9.2. The concentration of Mn^{2+} in the samples was determined after filtering through a cellulose membrane of 0.45 mm and quantified in an atomic absorption spectrophotometer (AAS, Varian® AA spectra, Melborne, Australia). The absorbance was measured at a wavelength of 279.5 nm with a spectral bandwidth of 0.2 nm.

2.1. Methods for Characterizing Biosorbents

The Moringa pods were collected in the city of Aracajú-SE/Brazil. The pods were then separated from the seeds, washed to remove dirt, and dried in a drying room at 60 °C for 24 h. After drying, the material was standardized to a particle size of 0.32 mm, and this material was then called the natural pod (untreated) (Pod_{NA}). The pod shell and the pretreated pods (Pod_{AC} and Pod_{BA}) were characterized before and after the biosorption process by infrared spectroscopy (FTIR) and scanning electron microscopy (SEM, Quanta FEI –250, Pantelimon, Roménia). The scanning electron microscopy with EDS microprobe (SS 550 Superscan Model, Shimadzu®, Kyoto, Japão) was used to study the surface morphology of biosorbents and their composition. Fourier transform infrared (FTIR) spectra were recorded by a Vertex 70v Bruker spectrophotometer, using the wavelength range of 4000–400 cm^{-1}. The FTIR spectrometry analyses were performed using KBr pellets, prepared in a ratio of 1/100 m/m.

The Point of Charge Zero (PCZ) was determined for all biosorbents to identify the pH at which the adsorbent surface changes. The methodology used for the determination was proposed by Wang et al. [36], where 0.1 g of adsorbent was added to 50 mL of distilled water at different initial pH conditions, ranging from 1 to 12. The flasks were shaken for 24 h at 25 °C and 200 rpm. After this period, the samples had their final pH measured and graphically compared with the initial pH values. The acid solutions were adjusted to 0.1 mol L^{-1} of HCl, and the bases to 0.1 mol L^{-1} of NaOH. The final pH (pHf) was measured. The graph showing the difference [ΔpH (pHf − pHi)] between the final and initial pH (pHi) was plotted and presented in the results section. The PCZ corresponds to the pH value where the curve crosses the x-axis [29].

2.2. Biomass Modification

Initially, the pods' shells (Figure 1) were separated from the Moringa seeds, crushed, washed with distilled water, and dried in a circulating oven at 60 °C until a constant weight, being called pod shell *in natura* (Pod_{NA}).

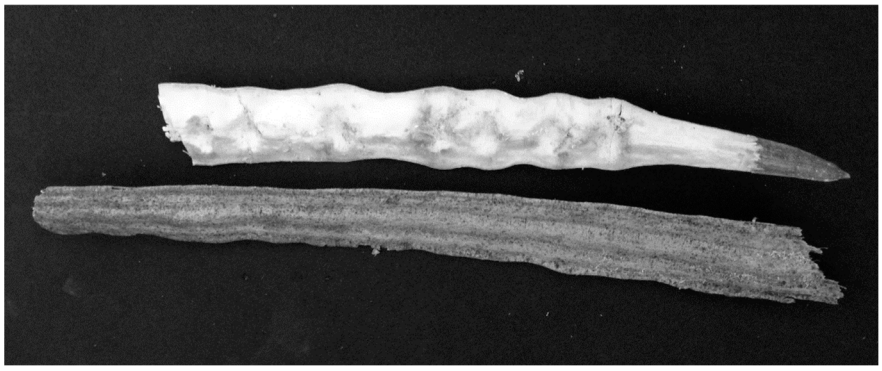

Figure 1. *Moringa oleifera* pod shell.

The pod modification was performed using the methodology described by Kumar and Gaur [29], where the evaluated treatment agents were NaOH (0.1 mol L^{-1}, Synth®, 97% purity) and HCl (0.1 mol L^{-1}, Synth®, 36.5% purity). Since the chemical pre-treatments

can potentially modify the cell surface by either removing or masking groups or exposing more metal ion binding sites, these agents were selected due to their known capacity for improving adsorption [37].

For the basic treatment, Pod_{NA} was added to the 0.1 mol L^{-1} NaOH solution in a 3:1 (NaOH volume/Moringa mass) proportion, agitated at 80 rpm for 30 min at 25 °C. Next, the biomass was centrifuged (300 rpm, 15 min), and the supernatant was discarded. The pellet formed was then washed with Milli-Q water to ensure the removal of excess base. The treated pod was dried in an oven at 60 °C to constant weight. After drying, the material was subjected to particle size patterning with a range of 0.1–0.32 mm, and its manganese removal ability by adsorption was evaluated. This material received the name basic-treated pod (Pod_{BA}). The same procedure was repeated for the treatment agent HCl 0.1 mol L^{-1}, giving rise to the material named acid-treated pod (Pod_{NA}).

2.3. Biosorption Experiments

The biosorption experiments were conducted in batch using a sealed plastic flask containing 50 mL of a Mn^{2+} solution at a concentration of 4 mg L^{-1}, with a stirring speed of 200 rpm in a thermostatic bath. The parameters evaluated during the adsorption tests were contact time, pH, temperature, and adsorbent mass, with each parameter varied individually.

The effect of the contact time was evaluated by varying the time from 2 to 150 min. A flask containing a Mn^{2+} solution (4 mg L^{-1}) and 0.5 g of biosorbent was stirred at 200 rpm in a thermostated bath at 25 °C for different periods, starting at a pH of 6 (the natural pH of the solution). Finally, the material was filtered through a 0.45 μm cellulose membrane, and aliquots were collected for quantification of metal concentration. A time of 60 min was established as the optimum time for use in subsequent experiments.

The influence of pH was studied by balancing the initial solution (Mn^{2+}, 4 mg L^{-1}) with NaOH (0.1 mol L^{-1}) and HCl solution (0.1 mol L^{-1}) for different pH (1.0, 3.0, 5.0, 6.0, 7.0, and 8.0), setting a fixed agitation speed of 200 rpm, adsorbent mass of 0.5 g, a temperature of 25 °C and 60 min.

The effect of adsorbent mass was investigated by varying the mass to 0.5, 0.7, 1.0, and 1.3 g. The experiment was conducted with a Mn^{2+} concentration of 4 mg L^{-1}, a stirrer speed of 200 rpm, a 60 min contact time, and a temperature of 25 °C, and the optimum pH was determined.

To evaluate the temperature effect, the parameters of metal concentration and rotation were maintained, using 0.5 g of adsorbent mass, an optimal pH was found, and the temperature was varied at 15, 25, 35, and 45 °C with a contact time of 60 min.

The biosorption experiments were performed in triplicate, and the results were expressed as mean ± standard deviation.

After establishing contact time, Mn^{2+} concentration was measured using AAS. The Mn^{2+} removal rate was calculated using Equation (1):

$$Mn^{2+}\ \text{Removal}\ (\%) = \left(\frac{(Co - Cf)}{Co}\right) \times\ 100 \quad (1)$$

The quantity of metal adsorbed by biomass in equilibrium was calculated using Equation (2).

$$q = (Co - Ce) \times V/m \quad (2)$$

where Co is the solute concentration in the initial solution (mg L^{-1}); Cf is the final residual metal concentration after the absorption period in mg L^{-1}; Ce is the final solute concentration in equilibrium (mg L^{-1}); V is the solution volume (L); and m is the adsorbent mass (g).

For the study of Mn^{2+} adsorption isotherms by biosorbents, optimal conditions were applied to each adsorbent, ensuring a balance in the system. The concentration of manganese ions was based on Abdeen et al. [22], which varied from 5 to 50 mg L^{-1}; the solutions after adsorption were then filtered through a cellulose membrane with a pore size of 0.45 µm, and the metal ions were quantified using an atomic absorption spectrophotometer. In this study, we applied two widely used isotherms, Langmuir and Freundlich; Equations (3) and (4) indicate these models, respectively.

The Langmuir model [38] used to evaluate the adsorption nature is expressed as

$$qe = \frac{qmax\ K_L\ Ce}{1 + K_L Ce} \quad (3)$$

In Equation (3), Ce (mg L^{-1}) refers to the equilibrium Mn^{2+} concentration, qe (mg g^{-1}) is the quantity of metallic ions adsorbed by mass unit of adsorbent in equilibrium state, qmax (mg g^{-1}) is the maximum capacity of adsorption, and K_L (L mg^{-1}) is the Langmuir constant [38].

The indicator in the Langmuir model, corresponding to the degree of development of the adsorption process, R_L, was calculated using the results obtained for qmax and K_L. The R_L value is obtained from Equation (4), shown below.

$$R_L = \frac{1}{1 + K_L Co} \quad (4)$$

The Freundlich equation can be described as

$$qe = K_f Ce^{1/n} \quad (5)$$

where K_f and n are Freundlich constants related to the adsorption capacity and adsorption intensity, respectively, across multiple layers. If the n-values were held within 1–10, it indicates that the biosorption process is suitable. For n values of 1, the adsorption is linear. Therefore, values lower than *n* indicate that chemical interactions favored adsorption; values greater than *n* characterize the favor of adsorption via physical processes [39].

To evaluate the kinetics of Mn^{2+} removal, pseudo-first-order and pseudo-second-order kinetic models were used to understand the biosorption dynamics of adsorbents Pod_{NA}, Pod_{AC}, and Pod_{BA}.

The pseudo-first-order kinetic model, as proposed by Lagergren [40], is presented below (Equation (6)).

$$Q_t = Q_e\left(1 - e^{1k_1 t}\right) \quad (6)$$

where Qt (mg g^{-1}) is the quantity of metallic ions adsorbed at moment t, and k_1 (min^{-1}) is the pseudo-first-order adsorption process constant.

The pseudo-second-order kinetic equation [41] is expressed in Equation (7).

$$Q_t = \frac{k_2\ Q_e^2 t}{1 + k_2 Q_e t} \quad (7)$$

Here, Q_e stands for the equilibrium adsorption capacity (mg g^{-1}) and k_2 (g mg^{-1} min^{-1}) is the pseudo-second-order adsorption rate constant.

3. Results and Discussion

3.1. Biosorbents Characterization

The characterization of the biosorbent surface and structure is important for understanding the mechanism of interaction between the biomass and the metal [42]. For

characterizing and analyzing the composition of surfaces, techniques such as scanning electron microscopy (SEM) with microprobe EDS (Energy-Dispersive Spectroscopy) and FTIR analysis were employed.

EDS (Table 1) analysis of the biosorbents (Pod_{NA}, Pod_{AC}, and Pod_{BA}) after Mn^{2+} biosorption reveals the incorporation of manganese into the samples, as none of the adsorbents initially contained Mn^{2+} in their composition. The presence of Mn^{2+} in the samples after the adsorption process confirms the pod's ability to adsorb metals.

Table 1. Elemental analysis of biosorbents obtained for EDS after adsorption.

Biosorbents	Element (%)					
	C	O	Mg	Al	Ca	Mn
Pod_{NA}	53.79	45.51	0.14	0.11	0.26	0.19
Pod_{AC}	53.93	45.11	0.0	0.12	0.29	0.55
Pod_{BA}	52.00	47.39	0.13	0.12	0.18	0.18

Tavares et al. [43] used Moringa pod shell as a biosorbent for removing lead from aqueous solutions. In his study, the author used EDS analysis to determine the elemental composition of the pod shell, and the result presented reveals a content of 54.44% carbon, 44.96% oxygen, and 0.60% trace elements (H, Mg, Na, K, Ca, Al, P, and S). These results confirm that the pod shell contains no manganese, and therefore, all the manganese present is due to biosorption.

Furthermore, the different values in the elemental composition for the different biosorbents may be due to the treatments applied. According to Kron et al. [44], alkaline treatment, for example, can alter the structure of cellulose.

Reddy et al. [45], working with moringa shells, report that compounds present in moringa, such as cellulosic structures and proteins, promote bonding with metals. This is because the metal ion is associated with functional groups present on the biosorbent surface, thereby favoring the biosorption process in Moringa.

Figure 2 shows the SEM images of the superficial morphology of adsorbents Pod_{FS}, Pod_{AC}, and Pod_{BA}.

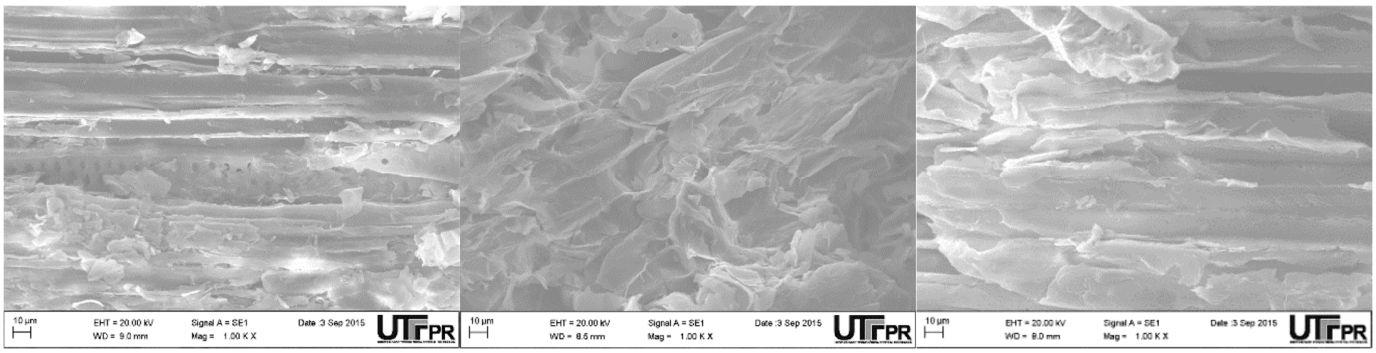

(**A**) (**B**) (**C**)

Figure 2. SEM micrographs of adsorbents: (**A**) In-natura pod (Pod_{NA}), (**B**) Acid-treated pod (Pod_{AC}), and (**C**) Basic-treated pod (Pod_{BA}).

By analyzing Figure 2, the adsorbents have a surface with a fibrous and heterogeneous appearance, irregular pores of varying dimensions, and are relatively open and asymmetrical. Such features can facilitate the metal biosorption process [33].

FTIR analysis is an effective method for obtaining information about the functional groups present on a material's surface. Figure 3A,B show the FTIR spectra of Pod_{NA}, Pod_{AC}, and Pod_{BA} pods.

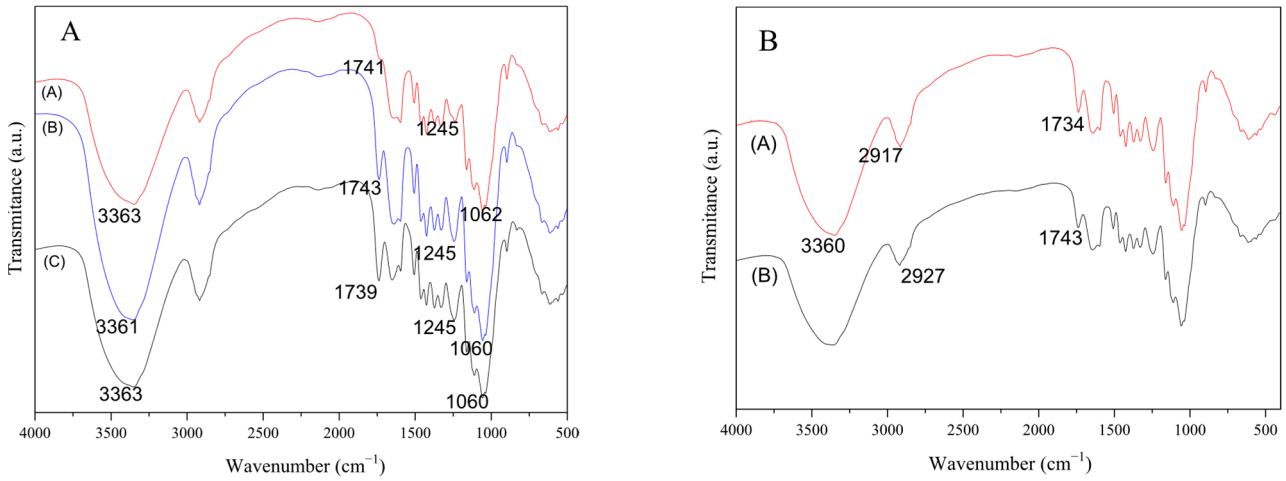

Figure 3. (**A**) FTIR pod spectrum: (A) Pod_{BA}, (B) Pod_{NA}, and (C) Pod_{AC}. (**B**) FTIR spectrum of (A) In-natura pod and (B) FTIR spectrum of in-natura pod after manganese adsorption.

Using the FTIR technique, the main functional groups present in the samples were identified. As it is a lignocellulosic material, there are many organic functional groups along the spectrum. The peaks at 2923 and 2852 cm^{-1} represent the C–H stretching attributed to the alkanes [46].

Figure 3A shows a broad band at 3360 cm^{-1}, assigned to the O-H stretching vibration. The peak present at 2923 cm^{-1} is attributed to the symmetric and asymmetric stretch of CH_2; this functional group is present in fatty acids, proteins, cellulose, hemicellulose, and lignin [42]. The peaks in the region of 1740 to 1630 cm^{-1} exhibit a change in intensity, indicating potential changes in the C=O bonds during the proposed treatments. The basic and acid treatments may cause hydrolysis reactions, resulting in the formation of new carboxylic groups (-COO) and hydroxyls (-OH) in the biomass, which can favor metal biosorption [37]. The spectral region of 1224 to 1248 cm^{-1} confirms the presence of carboxylic acids, which is associated with the C-O bond stretching in phenols [33]. The peak at 1054 cm^{-1} is assigned to C-O type bonds, confirming the presence of a lignin structure that contains functional groups such as hydroxyl and carbonyl, with the capacity to form interactions with metals and remove them. The peak at 893 cm^{-1} is attributed to C-O bonds, characteristic of the presence of cellulosic structures such as hemicellulose and cellulose [47,48].

Pretreatment promotes the presence of active functional groups such as hydroxyl (-OH) groups and carboxylic groups (-COOH), which are known to promote metal adsorption.

To verify the influence of manganese adsorption on the biosorbent, FTIR analysis was carried out on the in-natura biomass (Pod_{NA}), before and after Mn biosorption. These results are shown in Figure 3B. The spectra show an intense band at 3360 cm^{-1}, indicating the presence of hydroxyl groups. The presence of a peak at 2927 cm^{-1} (before adsorption) and 2917 cm^{-1} (after adsorption) can be attributed to the symmetric and asymmetric stretching of the C-H bond. The displacement of the peak after adsorption may indicate the binding of the metal to the surface of the biosorbent. Changing the wave number of the carbonyl band from 1743 cm^{-1} to 1734 cm^{-1} after the adsorption process indicates the possible connection of metal groups to carboxylic groups. Reddy et al. [45] worked with biomass of *Moringa oleifera* modified leaves as adsorbents for Cd(II), Ni(II), and Cu(II) removal, reporting a similar behavior for their adsorbent, where they claim that such modification is related to the interactions occurring between the carboxylic and hydroxyl groups with metals in solution.

According to Basu et al. [49], an offset band or a spectral region change is related to the metal bonding with the functional group involved. In this study, the regions where changes were identified after biosorption, when compared to the spectrum before biosorption of Mn^{2+}, were related to hydroxyl functional groups (3360 cm^{-1}) and carbonyl (1734–1743 cm^{-1}).

The subtle shift in the spectra before and after the adsorption process can be associated with the fact that the metal ion concentration is relatively low compared to the adsorbent mass in the adsorption process, which ultimately provides the non-appearance of new peaks and spectrum distortion, characterizing a mild physical adsorption process [37,45].

3.2. Determination of pH (pH_{PCZ}) at Zero-Charge Point (PCZ)

The pH (pH_{PCZ}) at which the surface of adsorbents is electrically neutral is known as the PCZ. Determining the biosorbent point of charge zero is crucial for elucidating the biosorption mechanism. Figure 4 shows the PCZ analysis of the studied biosorbents.

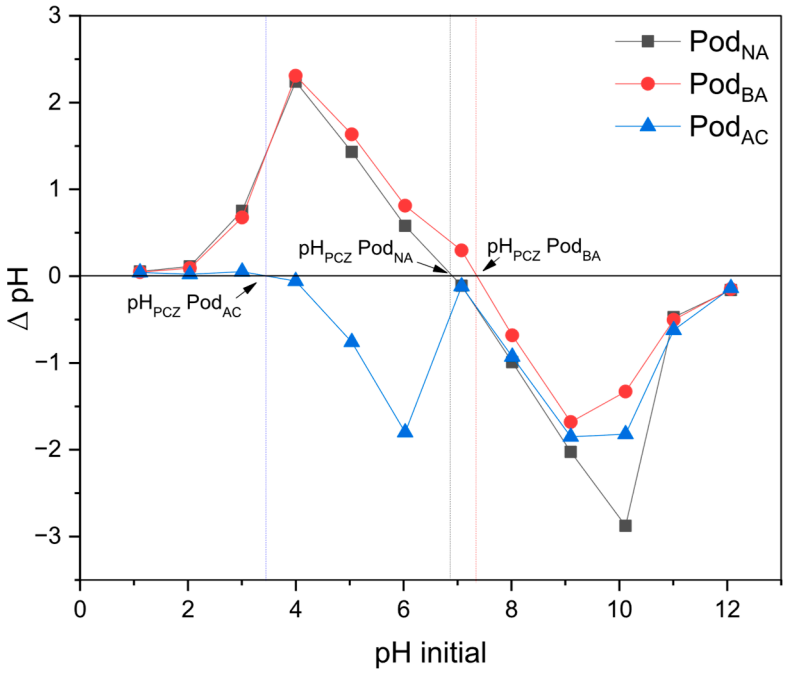

Figure 4. PCZ analysis for the Pod_{NA}, Pod_{AC}, and Pod_{BA} biosorbents. Conditions: Co = 4 mg L^{-1}; V = 50 mL; m = 0.5 g; T = 298 K; t = 60 min.

The pH_{PCZ} values were 6.9 for Pod_{NA}, 3.5 for Pod_{AC}, and 7.4 for Pod_{BA}. The results obtained in this work are close to those found by Tavares et al. [43], where the PCZ values obtained for Moringa pods without chemical functionalization were 6.9, 7.2 for the pod with basic treatment and 3.5 for the pod with acid treatment.

This indicates that the biosorbents acquire a positive charge below the PCZ range, and above this value, they acquire a negative charge. At zero charge point, the electrostatic forces between the dissolved Mn ions and the surface of the adsorbent are balanced, so that their charges are canceled. As pH < pH_{PCZ}, the biosorbent exhibits a positive surface charge, leading to electrostatic repulsion of Mn, which reduces its adsorption capacity. When pH > pH_{PCZ}, the biosorbent surface charges become negative, thereby attracting Mn ions in solution to the surface, which favors adsorption. Reddy et al. [45] reported that metal adsorption is related to both the pH and the nature of the biosorbent, since each biomass has its optimum pH for metal ion adsorption. Thus, different behaviors provide a preliminary indication of the adsorbent's behavior at varying pH levels.

Owing to electrostatic attraction, negative and positive surfaces of adsorbents are conducive to the adsorption of positive and negative ions, respectively [29]. The biosorption process may take place through different mechanisms, such as ion exchange, chelation, and physisorption.

These mechanisms usually involve surface functional groups that, in aqueous media, are responsible for the capture and retention of metal species. pH variations can alter these groups, thereby influencing the efficiency of the biosorption process [43].

3.3. pH Influence in the Biosorption Process

The effect of pH on manganese adsorption for the adsorbents Pod_{NA}, Pod_{AC}, and Pod_{BA}, with pH ranging from 1 to 8, is graphically represented in Figure 5.

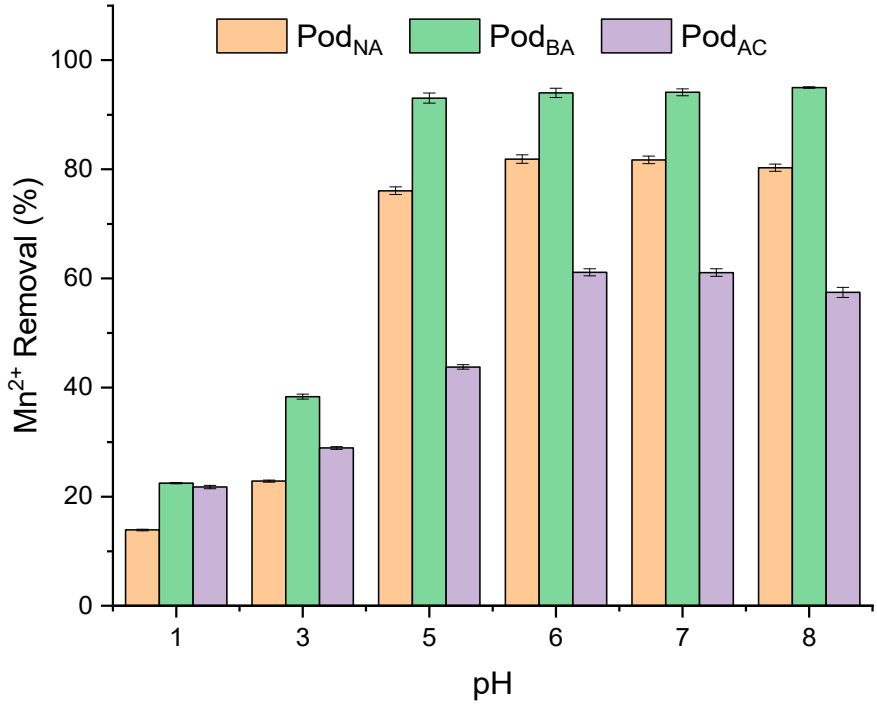

Figure 5. Effect of pH on manganese adsorption for the adsorbents: Pod_{NA}, Pod_{AC}, and Pod_{BA}. Conditions: Co = 4 mg L^{-1}; V = 50 mL; m = 0.5 g; T = 298 K; t = 60 min.

In the adsorption process, the pH of the solution is an important variable, as it directly affects metal sorption due to the protonation/deprotonation of the adsorbent's functional groups [20].

It is worth noting that the removal capacity for acid-treated pods, in-natura pods, and basic-treated pods initially increased with the pH and then remained broadly unchanged from pH 6.0 onwards. The maximum removal was observed in the pH 6–8 range for the three biosorbents studied; therefore, the pH chosen for further studies was six, as this value showed good removal for all biosorbents and is the natural pH of the solution. For the Pod_{NA} biosorbent, the removal percentages were around 61% for pH 6 and 7, and for the Pod_{AC} biosorbent, the removal percentages were ≅ 81% for the same pH values. The Pod_{BA} biosorbent showed a removal percentage of 94% for the pH 6–8 range. A study conducted by Cardoso et al. [27] investigated the potential of coconut shell powder derived from *Cocos nucifera* agricultural waste as a sustainable biosorbent for removing Mn^{2+}. The study found that the maximum removal efficiency of Mn^{2+} was 86.4% at pH 7.

This data shows that natural pH values of water, between pH 6 and 7, can be used efficiently to remove Mn^{2+} when using these biosorbents.

The behavior of the adsorbents Pod_{NA}, Pod_{AC}, and Pod_{BA} for the removal of Mn^{2+} (revealing that the optimum pH value for biosorbents in removing Mn^{2+} in solution was 6.0) ions in solution confirms the PCZ principle, where manganese adsorption is favored at higher pH values than those found in the zero charge point study.

The Pod_{AC} adsorbent's performance in removing Mn^{2+} from solution confirms the data obtained in PCZ analysis, where manganese adsorption is favored at higher pH values. As for Pod_{NA} and Pod_{BA}, removal was favored in the zero-load range. Variations in metal sorption at different pH levels can be related to the ionic strength [50]. Furthermore, the alkaline treatment can contribute to the exposure of specific chemical groups by reinforcing the connection between the cation and the metal adsorbent [37]. Another factor to consider is that on the PCZ, the adsorbent surface charge tends to be neutral, allowing electrostatic forces between metal ions and the adsorbent surface to equilibrate. Even in equilibrium, certain carboxylic and hydroxyl groups present in the sorbent molecule remain available for connecting with metals [51].

3.4. Biosorbent Dose Effect

The Mn^{2+} biosorption by the studied adsorbents (Pod_{NA}, Pod_{AC}, and Pod_{BA}) was evaluated by varying the adsorbent amount from 0.5 to 1.5 g in solution, with an initial concentration of 4 mg L^{-1}, pH 6, and a contact time of 60 min. The effect of the biosorbent dose on Mn^{2+} adsorption is shown in Figure 6.

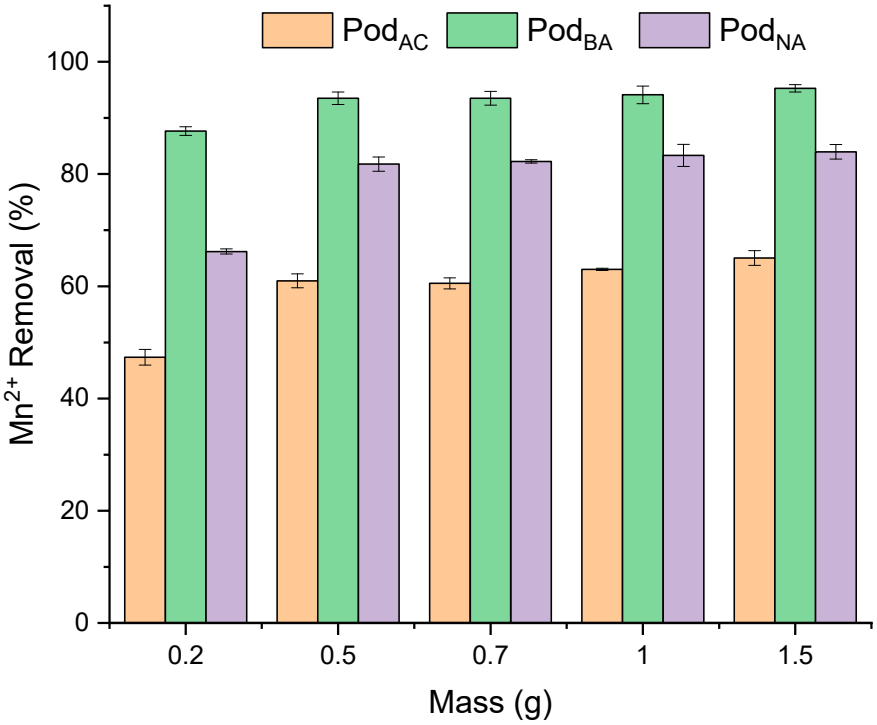

Figure 6. Biosorption dose effect in Mn adsorption of Pod_{NA}, Pod_{AC}, and Pod_{BA}. Conditions: Co = 4 mg L^{-1}; V = 50 mL; pH = 6; T = 298 K; t = 60 min.

The in-natura pod demonstrated a satisfactory removal capacity; therefore, for the pre-treatments, the alkaline treatment showed better removal than the acid treatment. The removal percentage varied from 66% to 83% with the in-natura pod, from 47% to 65% with the acid-treated pod, and from 87% to 95% with the basic-treated pod. Obtaining a residual manganese in solution of 0.68 mg L^{-1}, 1.4 mg L^{-1}, and 0.2 mg L^{-1}, respectively, for the Pod_{NA}, Pod_{AC}, and Pod_{BA} pods. This result can be explained by the fact that increasing the amount of biomass, the surface area, and the number of active sites available for new

connections increases, improving the bioremediation capacity [22]. Furthermore, Lalhruaitluanga et al. [39] reported that alkali biomass pretreatments improve the adsorption capacity compared to untreated biomass, as they may contribute to the availability of specific functional groups responsible for anchoring metals, thereby enhancing the biomass's adsorption capacity.

3.5. Kinetic Study

Considering the optimal dosage of adsorbent (0.5 g) and pH (6.0), the adsorption kinetics were performed under these conditions for 60 min. The kinetic models, PFO and PSO, were fitted to the experimental data (Figure 7), and their corresponding parameters are presented in Table 2.

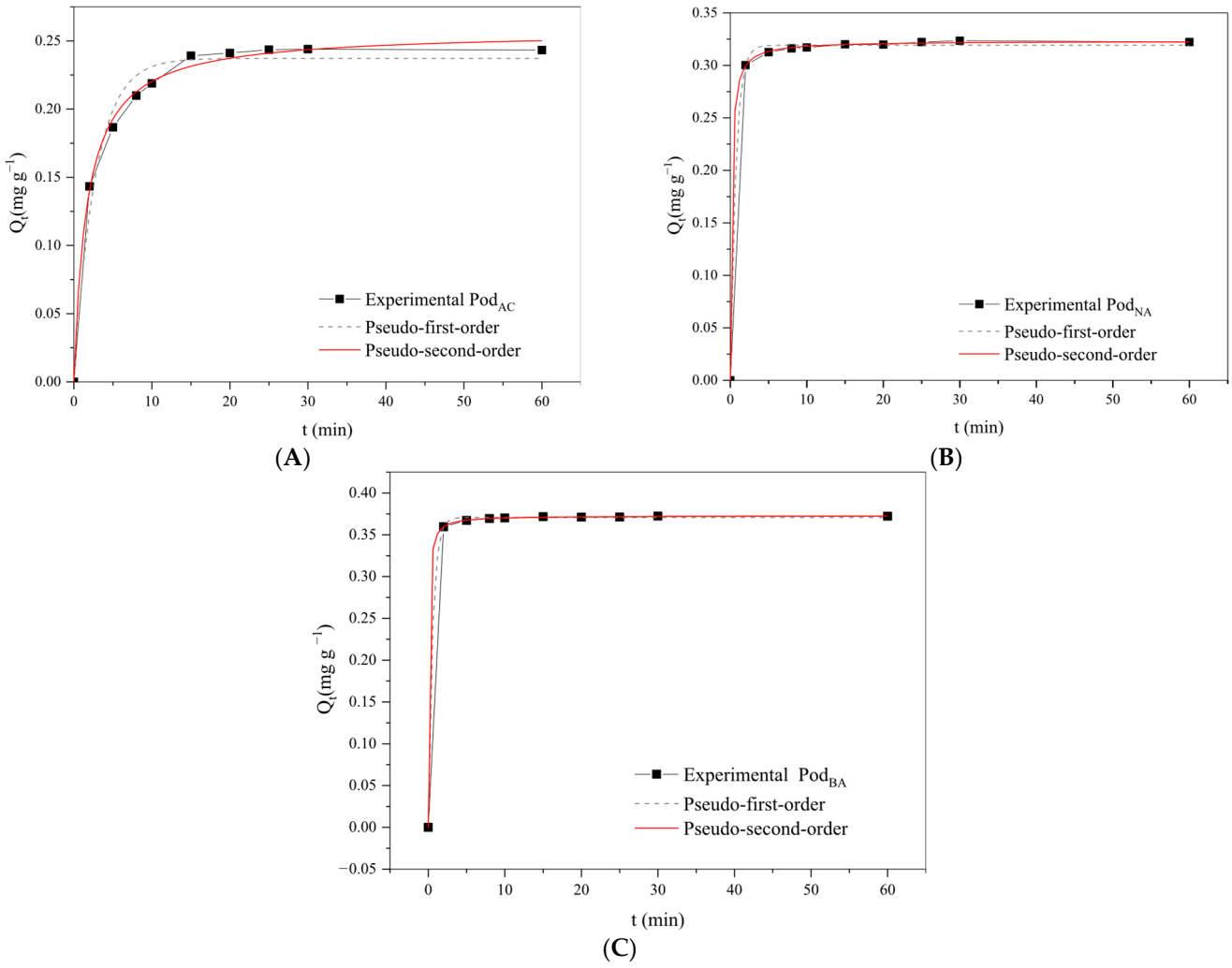

Figure 7. Mn^{2+} biosorption kinetic data of (**A**) Pod_{NA}, (**B**) Pod_{AC}, and (**C**) Pod_{BA} were fitted to the pseudo-first-order and pseudo-second-order mathematical models. Conditions: Co = 4 mg L^{-1}; V = 50 mL; m = 0.5 g; T = 298 K; pH = 6.

Analyzing Figure 7, it can be noticed that the adsorption percentage increases with contact time until equilibrium is reached. The kinetic study of the three adsorbents (Pod_{NA}, Pod_{AC}, and Pod_{BA}) in removing Mn^{2+} from solution showed that they exhibit similar adsorptive behavior, with most of the metal ions being removed within a range of 2–30 min. It was observed that for the biosorbents Pod_{BA} and Pod_{NA}, the maximum adsorption capacity of Mn^{2+} was reached with only 5 min of operation due to the affinity and availability of large numbers of vacant binding sites on the biosorbent surface. For the biosorbent

Pod_{AC}, the equilibrium time was slightly longer, at 20 min. This relatively short equilibrium time aligns with other authors who used biomass for the removal of Mn^{2+} from aqueous solutions. Vera et al. [24] determined an equilibrium time of less than 20 min, and Dal-Bó et al. [29] achieved over 97% adsorption in 15 min. However, other biosorbents may exhibit much longer equilibrium times, such as the fruit bunch oil palm biochar used by Savitri et al. [28], with at least 24 h of adsorption, while the macaúba used by Giraldo-Bareño et al. [26] reached equilibrium only after 48 h of adsorption.

Table 2. Kinetic parameters of biosorbents Pod_{NA}, Pod_{AC}, and Pod_{BA} during the Mn ion biosorption process.

Biosorbents	Q_{eexp} (mg g^{-1})	Pseudo-First-Order		
		$Q_{t\ cal}$ (mg g^{-1})	K_1 (min^{-1})	R^2
Pod_{NA}	0.327	0.319 ± 0.001	1.403 ± 0.093	0.998
Pod_{AC}	0.243	0.237 ± 0.005	0.366 ± 0.042	0.979
Pod_{BA}	0.374	0.371 ± 0.001	1.753 ± 0.076	0.999
		Pseudo-Second-Order		
Pod_{NA}		0.323 ± 0.00	19.561 ± 1.097	0.999
Pod_{AC}		0.253 ± 0.003	2.329 ± 0.197	0.996
Pod_{BA}		0.373 ± 0.000	36.449 ± 1.250	0.999

Conditions: C_o = 4.0 mg L^{-1}; T= 298 K; V = 50 mL; m = 0.5 g; pH = 6.

The maximum biosorption was 81.70% for Pod_{NA}, 60.97% for Pod_{AC}, and 93.85% for Pod_{BA}, indicating residual manganese in solution of 0.732 mg L^{-1} for the in-natura pod, 1.561 mg L^{-1} for the acid-treated pod, and 0.246 mg L^{-1} for the basic pod. After the treatment, the biomass undergoes a series of changes, including the removal of surface impurities, membrane rupture, and the exposure of new functional groups, such as hydroxyls and carboxylic groups, which may favor or hinder the biosorption process [37].

It can be seen that for the acid-treated pod, equilibrium was reached in a longer time than for the other adsorbents. This corroborates the lower percentage of adsorption, demonstrating greater difficulty in the adsorption process for this adsorbent.

Ideally, in drinking water treatment plants, shorter contact times are favorable as this implies more batches can be processed in each time interval, ultimately reducing operational costs and operating time [24].

As shown, the Mn^{2+} removal increases significantly in the initial phase, reaching equilibrium within approximately 30 min for the three adsorbents studied; however, a longer time was chosen to obtain the adsorption isotherm (60 min), ensuring the system had reached equilibrium.

As shown in Table 2, the pseudo-second-order model is the one that best describes the biosorption of Mn^{2+} by moringa pods. The Pod_{NA} and Pod_{BA} biosorbents presented the most significant R^2 coefficient values, 0.999, and values closer to Q_{eexp} and Q_{tcal}, reinforcing the applicability of this model. The second-order kinetic model suggests that the limiting rate stage was chemisorption, indicating that the adsorption process is dependent on the amount of adsorbed metal ions on the adsorbent surface and the amount adsorbed at equilibrium [51]. These results are consistent with Cardoso et al. [27] and Carmo et al. [35], who found that the pseudo-second-order model effectively described the adsorption of Mn ions using coconut shell powder biosorbent and Moringa seeds, respectively.

As discussed in the FTIR analysis, the carboxyl and hydroxyl groups found in the adsorbents, and more available in the Pod_{BA} adsorbent, can act in the adsorption process, favoring the removal of the metal from aqueous solutions.

3.6. Equilibrium Isotherms

The experimental data fitted to the Langmuir and the Freundlich experimental models are shown in Figure 8.

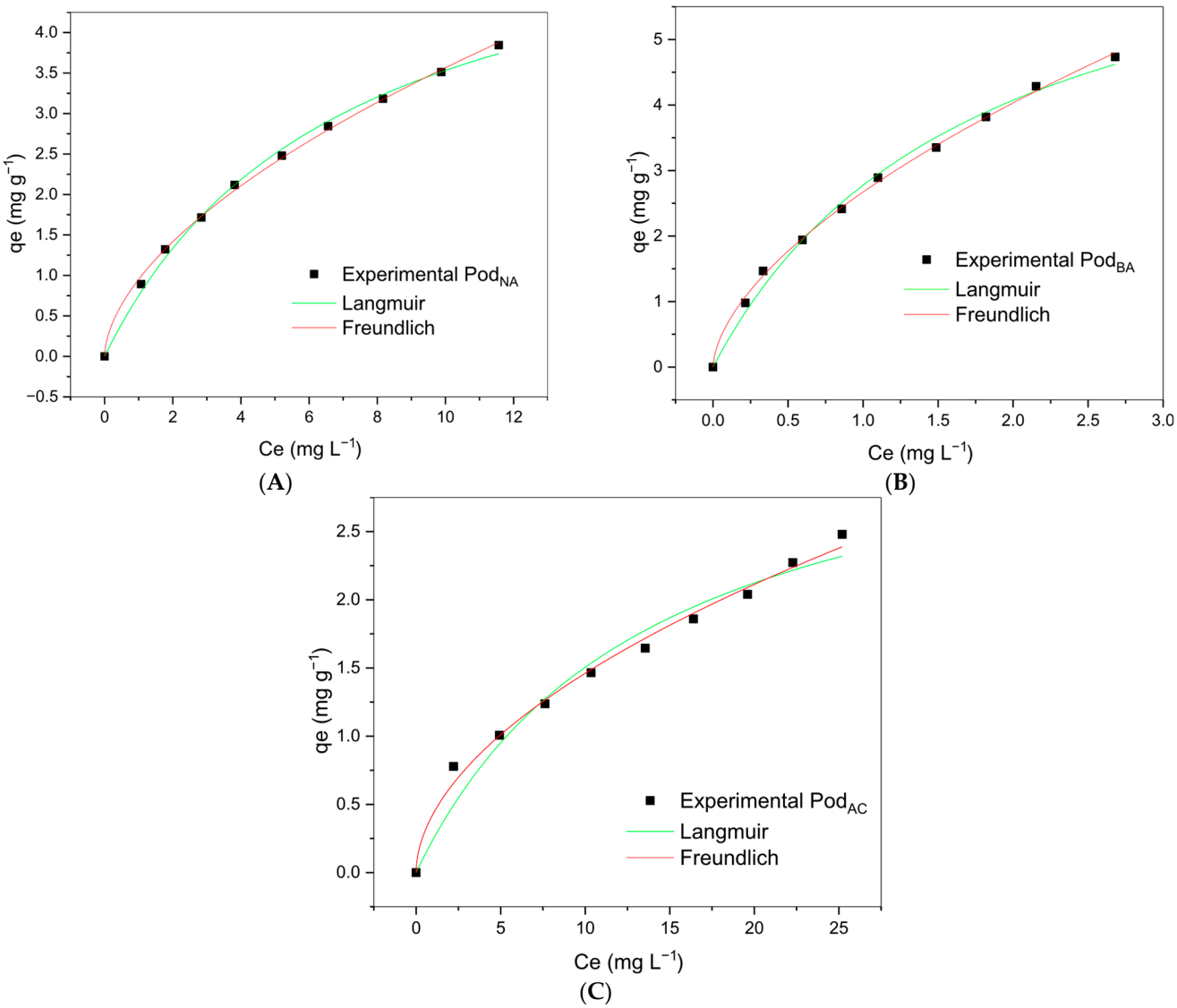

Figure 8. Langmuir and\Freundlich isotherms adjusted to manganese ion adsorption experimental data for Pod_{NA} (**A**), Pod_{AC} (**B**), and Pod_{BA} (**C**) adsorbents. Conditions: Co =10 to 50 mg L^{-1}, V = 50 mL, m = 0.5 g, T = 298 K, pH 6, t = 60 min.

The adsorption isotherm expresses the relation between the biosorbent amount per gram of adsorbed metal ions, in addition to providing information on the adsorption behavior [22]. Several isothermal models have been widely used to determine a model for the system equilibrium adsorption. The most commonly used models are the Langmuir and the Freundlich, where the Langmuir adsorption model assumes that it occurs over a homogeneous monolayer surface without any interaction between the adsorbed ions. The adsorbed molecules occupy a single site, and the adsorption ends when all sites are occupied, forming an adsorbate monolayer on the surface of the adsorbent [28,29].

On the other hand, the Freundlich equation is an empirical model based on adsorption onto a heterogeneous surface, implying that adsorption occurs in multiple layers, where the energy diminishes exponentially with increasing surface coverage.

The accuracy of model fit was determined using statistical measures such as correlation coefficient (R^2) and chi-square (χ^2) values. The model with the lowest χ^2 and a high R^2 was selected. The parameters obtained for each model are given in Table 3.

Table 3. Parameters of the isotherms adjusted to the Langmuir and the Freundlich models for Mn^{2+} adsorption.

Biosorbents	Langmuir				
	q_{max} (mg g^{-1})	K_L (L mg^{-1})	R_L	χ^2	R^2
Pod_{NA}	6.001 ± 0.249	0.142 ± 0.012	0.123	0.006	0.996
Pod_{AC}	3.601 ± 0.422	0.072 ± 0.018	0.218	0.019	0.967
Pod_{BA}	7.645 ± 0.504	0.570 ± 0.072	0.034	0.017	0.992
Biosorbents	**Freundlich**				
	Kf ($mg^{1-1/n}$ $L^{1/n}$ g^{-1})	n		χ^2	R^2
Pod_{NA}	0.950 ± 0.023	1.741 ± 0.036		0.002	0.998
Pod_{AC}	0.429 ± 0.032	1.877 ± 0.941		0.004	0.992
Pod_{BA}	2.671 ± 0.024	2.671 ± 0.023		0.004	0.998

As shown in Table 3, the experimental data for Pod_{NA}, Pod_{AC}, and Pod_{BA} biosorbents were well-fitted by the Langmuir and the Freundlich models, with higher R^2 values for both Pod_{Na} and Pod_{BA}. It was also observed that the maximum adsorption capacity (q_{max}) was 7.645 mg g^{-1} for Pod_{BA}, 6.001 mg g^{-1} for Pod_{NA}, and 3.601 mg g^{-1} for Pod_{AC}. Comparing the maximum adsorption capacity qmax and maximum experimental adsorption capacity qmax values, it is possible to deduce that the maximum load capacity of Mn^{2+} in the biosorbent has not been reached with the experimental data from this study. This is probably due to the difference in the initial concentration of Mn^{2+} in the kinetic and equilibrium isotherm experiments. However, this data should not compromise the understanding that the studied biosorbents are effective options for the biosorption of Mn^{2+} from aqueous solution.

Giraldo-Bareno et al. [26], using a biosorbent chemically modified (with NaOH) macaúba (Acrocomia aculeata), found that the Langmuir model was the best fit for the experimental results, obtaining a qmax of 1.379 mg g^{-1} and a K_L of 0.016 L mg^{-1} for the removal of Mn ions. K_L value is a measure of adsorption affinity. In the present study, using the same type of basic treatment, higher values were obtained for qmax (7.645 mg g^{-1}) and K_L (0.570 L mg^{-1}). Dal-Bó et al. [29], using apple pomace biochar, reached values of qmax and de K_L of 1.449 mg g^{-1} and 4.082 L mg^{-1}, respectively. These results demonstrate the effectiveness of Moringa pod shells in removing Mn^{2+} from aqueous solutions.

An indicator commonly used in the Langmuir model, which corresponds to the degree of development of the adsorption process, is the R_L value (separation factor). In most adsorption situations, the adsorbate favors the solid phase over the liquid phase, and the adsorption is considered favorable when $0 < R_L < 1$. When $R_L > 1$, it indicates that the solute prefers the liquid phase over the solid phase. RL = 1 corresponds to a linear isotherm [52]. As can be seen in Table 3, the Pod_{BA} biosorbent showed the lowest R_L value, 0.034, indicating its higher affinity for the biosorbent and corroborating the data for greater Mn^{2+} adsorption capacity.

When analyzing the R^2 and χ^2 values together, a better fit of the experimental data to the Freundlich model is observed for the three biosorbents studied. These data are in agreement with other authors who used biosorbents for the removal of Mn^{2+} [30,51].

The Freundlich isotherm confirms the heterogeneity of the adsorbent surface sites, as the values of n are between 1 and 10, indicating that the biosorption of Mn^{2+} for the studied

adsorbents was favorable. Moreover, graphs show that the sorption did not achieve a limit value or the adsorbent saturation, indicating a multilayer adsorption process [53].

The alkaline treatment of lignocellulosic material is an irreversible process and leads to a change in the supramolecular structure and its morphology, facilitating its "solubilization". Two different cellulose chain structures (type I and type II) can be formed [44]. Thus, the increase in adsorption capacity in Pod_{BA} subjected to basic treatment can be attributed to the formation of type II cellulose, which has more available hydroxyl groups to react with the metal. These hydroxyl groups can be confirmed by the FTIR analysis shown in Figure 3B.

Thus, the maximum capacity results obtained for the Pod_{BA} biosorbent, which are higher than those of the other biosorbents [24,26,54], are in line with the above. The basic treatment proved to be the most efficient for manganese ion removal, achieving a 94% removal rate. However, the high manganese ion removal capacity indicates that the basic-treated moringa pod biosorbent is a promising treatment for metal removal.

The biosorption capacities of various biosorbents on manganese ion removal reported in the literature are shown in Table 4. When comparing the qmax values and removal percentages obtained experimentally with those reported in the literature for other adsorbents, it is clear that the adsorbents studied—PodNA, PodAC, and PodBA—have Mn ions removal capabilities that are similar to those found in previous studies. The results of this study showed that treated moringa pods demonstrate good Mn^{2+} removal properties from solutions; furthermore, pods offer a series of advantages in their use, such as low cost because it is a byproduct, renewability, biodegradability, and simplicity of treatment for obtaining the biosorbent.

Table 4. Biosorbents used for manganese removal.

Biosorbents	Mn^{2+} Removal Capacity (mg g^{-1})	References
Sugarcane bagasse	2.82	[24]
Bamboo biochar	5.0226	[18]
Commercial activated carbon	4.8355	[18]
Chitosan-impregnated bamboo biochar	5.2029	[18]
Iron-impregnated bamboo biochar	0.2170	[18]
Acid-treated corn cob	6.54	[22]
Pumice	0.519	[52]
Fe-pumice	7.148	[52]
Coconut shell powder	13.9	[27]
Palm waste-derived biochar	3.57	[51]
Macaúba endocarp treated with NaOH	1.379	[26]
Moringa seeds	10.35	[36]
Moringa pod shell in natura (Pod_{NA})	6.001	This work
Acid-treated Moringa pod shell (Pod_{AC})	3.601	This work
Basic-treated Moringa pod shell (Pod_{BA})	7.644	This work

Regarding the possible applications of manganese-saturated biosorbents, Vera et al. [24] suggest their use as fertilizer or pozzolanic material. According to the author, limit values for this metal are not provided by European Union directives and regulations for ashes used as forest fertilizer, as Mn (II) is a micronutrient element in soils. Therefore, the use of the ash as a soil conditioner can be an optimal option for its recycling and proper management after calcination, especially for soils deficient in manganese. The authors also mention the option of using it as an alternative pozzolanic material for concrete preparation, thus ensuring that the metals are not leached from these matrices.

3.7. Temperature Effect in Biosorption

With a contact time of 60 min, pH 6, and a fixed adsorbent dose of 0.5 g, the effect of temperature on the adsorption of Mn^{2+} per Pod_{NA}, Pod_{AC}, and Pod_{BA} was studied at temperatures ranging from 288 to 318 K. The effect of temperature variation is shown in Figure 9.

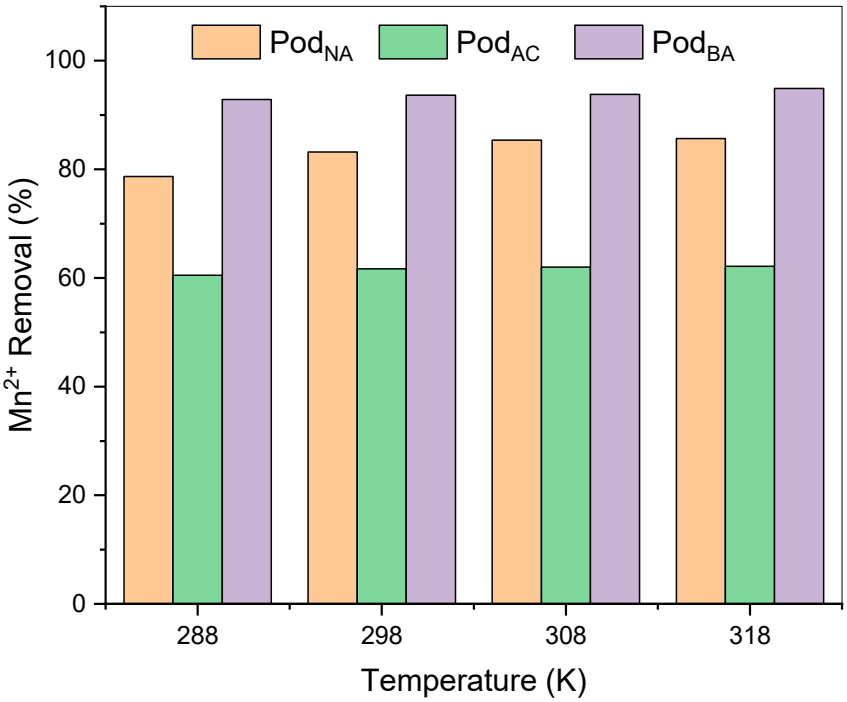

Figure 9. Temperature effect on Mn^{2+} removal capacity of Pod_{NA}, Pod_{AC}, and Pod_{BA}.

The removal ranged from 79% to 85% for Pod_{NA}, 61% to 62% for Pod_{AC}, and 92% to 94% for Pod_{BA}, resulting in residual manganese solutions of 0.6 mg L^{-1} for the in-natura pods, 1.52 mg L^{-1} for the acid-treated pods, and 0.24 mg L^{-1} for the basic-treated pods.

The results show that for all three adsorbents, biosorption is enhanced with increasing temperature. This fact is due to the endothermic nature of the adsorption process, whereas as the temperature rises, adsorption tends to increase. However, the temperature variation showed no significant difference in manganese biosorption capacity at 25 °C, which was chosen as the temperature for further studies. Tounsadi et al. [21], when working with *Diplotaxis harra* and *Glebionis coronaria* L. biomass for Cd (II) and Co (II) adsorption, observed that the temperature did not influence their adsorptive process. This fact is associated with the morphological nature of the biosorbent, which lacks defined pores, thereby not favoring the adsorption process.

3.8. Biosorption Thermodynamics

The temperature effect on the adsorption of Mn ions by the adsorbent was studied at 288, 298, 308, and 318 K with a constant concentration of 4 mg L^{-1}, pH 6.0, and a contact time of 60 min. The dependence of the equilibrium constant (Kc) for the Mn ions adsorption was calculated for all temperatures using Equation (8):

$$Kc = \frac{Fe}{1 - Fe} \quad (8)$$

where Fe is the percentage sorption fraction in equilibrium. The thermodynamic parameters, Gibbs free energy (ΔG°), enthalpy variation (ΔH°), and entropy variation (ΔS°) [43] were calculated using Equations (9) and (10):

$$\ln Kc = -\frac{\Delta H}{RT} + \frac{\Delta S}{R} \quad (9)$$

$$\Delta G^\circ = -RT\ln Kc \quad (10)$$

Here, R is the universal gas constant (8.314 J (mol K)$^{-1}$) and T is the absolute temperature (K). The values of ΔH° and ΔS° can be calculated using the intersection of ln Kc vs. 1/T rect. The thermodynamic parameters for the adsorption process using different biosorbents are presented in Table 5.

Table 5. Thermodynamic parameters used in Mn^{2+} adsorption for the different adsorbents are shown.

Biosorbent	ΔG°(kJ mol^{-1})				ΔH° (kJ mol^{-1})	ΔS° (J mol^{-1} K^{-1})
	288 K	298 K	308 K	318 K		
Pod_{NA}	−9.34	−12.18	−14.85	−15.71	11.88	52.10
Pod_{AC}	−1.08	−1.18	−1.25	−1.30	1.08	7.49
Pod_{BA}	−6.12	−6.64	−6.95	−7.67	8.94	51.61

The negative ΔG° values obtained at different temperatures for all adsorbents confirm the spontaneous nature of the reaction, as well as the viability of the biosorption process.

For ΔH° values found for all samples were positive, confirming the endothermic nature of the process. Furthermore, the enthalpy change value is indicative of physical or chemical processes, in which the heat involved during the physisorption process must be less than 40 kJ mol^{-1} [55,56]. Therefore, we can assure that the Mn^{2+} adsorption by Moringa pod shells involves physical adsorption mechanisms.

The analysis of the functional groups found on the surface of the adsorbents, together with the fit to the Freundlich kinetic model, is consistent with the thermodynamic analysis, indicating that the manganese adsorption process on moringa pod shells may occur by physisorption.

The positive entropy value indicates the system's tendency towards randomness during the adsorption process [22].

The data of an exothermic nature, with positive ΔH° and less than 40 kJ mol^{-1}, spontaneous, with negative ΔG° values, and a tendency to randomization, indicated by the positive ΔS° value, are in agreement with the literature. Vera et al. [24] studied the adsorption of Mn^{2+} on sugarcane bagasse, a cellulose-based adsorbent like Moringa pod shell, and found similar aspects in the thermodynamic analysis.

3.9. Adsorption Mechanisms

According to the characterization of Moringa pod shell and the adsorption studies of Mn^{2+}, it can be said that mechanisms of a physical nature govern the adsorptive process. The biomass biosorption per metal can be attributed to the presence of functional groups in the compounds of lignin, protein, carbohydrates, phenolics, etc., which contain carboxyl, hydroxyl, phosphate, and amino groups [33]. It is known that lignin, cellulose, and hemicellulose are the most important components of Moringa pod shell. It contains aromatic rings and functional groups that can form hydrogen bonds and π-interactions. Therefore, it is expected that these mechanisms are the main ones to explain the adsorption of Mn^{2+}.

Chemical modification has shown great promise in improving the adsorption and the cation exchange capacity of agricultural by-products. Reddy et al. [45] found that the pod shell with basic treatment exhibited the highest adsorption capacity.

The mechanisms associated with heavy metal biosorption by biomass are still not clear; however, it is important to note that this process is not based on a single mechanism. Metal sequestration occurs through complex mechanisms, including ion-exchange and complexation, and at least some of these mechanisms may act simultaneously to varying degrees depending on the biomass, the metal ion, and the solution environment [31].

Ion-exchange is an important concept in biosorption because it explains many of the observations made during heavy metal uptake experiments [55]. In this context, "ion-exchange" does not specify how heavy metals bind to biomass; instead, electrostatic or London–van der Waals forces (ionic and covalent bonds) are the actual chemical binding mechanisms [31].

The thermodynamic study determined an adsorptive process with ΔH° below 40 kJ mol^{-1}, describing physiosorption. Therefore, it can be said that the adsorption of Mn^{2+} onto Moringa pod shell is governed by mechanisms of a physical nature, which was confirmed by the pH and FTIR studies.

So, in general, it can be said that in the current biosorption process, there is deprotonation of the acidic sites (pH > 6), ion exchange/complexation of the biosorbent with Mn^{2+} at carboxylic and phenolic sites, and electrostatic alteration when the surface is negatively charged (pH > PCZ). The low uptake of Mn^{2+} at pH < 6 might be due to the electrostatic repulsion between the Moringa pod shell surface and Mn^{2+}. At slightly acidic to neutral pH, the deprotonation of -COOH generates $-COO^{-}$ sites capable of coordinating Mn^{2+}, while the overall negative charge of the surface favors electrostatic attraction of the cation. Thus, the removal of Mn^{2+} by Moringa pod shell occurs mainly through ion exchange and complexation at carboxylate and phenolic groups of the lignocellulosic matrix.

4. Conclusions

This study demonstrated that *Moringa oleifera* seed pods, particularly those chemically modified with NaOH, exhibit significant potential as biosorbents for Mn^{2+} removal from aqueous solutions. The alkali-treated biosorbent achieved a maximum adsorption capacity of 7.64 mg g^{-1}, compared to 6.00 mg g^{-1} for the untreated material and above most values found in the literature. Under optimized conditions, the process reduced the residual manganese concentration to 0.24 mg L^{-1} from an initial 4.00 mg L^{-1} (reduction of 94%), meeting the standards established by the U.S. EPA. Kinetic modeling confirmed that biosorption follows pseudo-second-order kinetics, and thermodynamic analysis indicated a spontaneous and physisorption-dominated mechanism. The ability to remove Mn^{2+} from aqueous solution is not trivial, given the large number of studies using different adsorbents available in the literature, which can be considered an important advance for the Moringa biosorbent. These findings validate the efficiency, feasibility, and sustainability of Moringa pods as renewable, low-cost, and biodegradable biosorbents, contributing both to environmental remediation and the valorization of agro-industrial residues.

Author Contributions: Conceptualization, A.M.S.V. and L.A.d.M.P.; methodology, L.A.d.M.P. and F.d.O.T.; investigation, L.A.d.M.P. and F.d.O.T.; data curation, L.A.d.M.P., F.d.O.T., A.M.S.V. and M.F.V. writing— original draft preparation, L.A.d.M.P. and F.d.O.T.; writing—review and editing, L.A.d.M.P.; project administration, A.M.S.V.; funding acquisition, A.M.S.V. and R.B. All authors have read and agreed to the published version of the manuscript.

Funding: This research was funded by Coordination for the Improvement of Higher Education Personnel (CAPES), financial code 001.

Data Availability Statement: The data are contained within the article.

Acknowledgments: The authors would like to thank the Graduate Program in Food Science at State University of Maringá, where this work was initially developed as part of the master's thesis entitled "Biossorção de Mn por vagem de *Moringa oleifera* a partir de águas contaminadas", defended in 2016. The authors would like to thank the Federal University of Technology—Paraná (UTFPR) for SEM micrographs.

Conflicts of Interest: The authors declare no conflicts of interest.

References

1. Salimi, A.; Ghanbarizadeh, P.; Mirvakili, A.; Moheimani, N.R. Optimizing heavy metal remediation of synthetic wastewater using Chlorella vulgaris and Sargassum angustifolium: A comparative analysis of biosorption and bioaccumulation techniques. *STOTEN* **2025**, *992*, 179938. [CrossRef]
2. Taffarel, S.R.; Rubio, J. Removal of Mn^{2+} from aqueous solution by manganese oxide-coated zeolite. *Miner. Eng.* **2010**, *23*, 1131–1138. [CrossRef]
3. Khan, M.U.; Malik, R.N.; Muhammad, S. Human health risk from Heavy metal via food crops consumption with wastewater irrigation practices in Pakistan. *Chemosphere* **2013**, *93*, 2230–2238. [CrossRef] [PubMed]
4. Rahman, M.S.; Molla, A.H.; Saha, N.; Rahman, A. Study on heavy metals levels and its risk assessment in some edible fishes from Bangshi River, Savar, Dhaka, Bangladesh. *Food Chem.* **2012**, *134*, 1847–1854. [CrossRef] [PubMed]
5. Joshia, P.; Bodnya, C.; Ilievab, I.; Neely, M.D.; Aschner, M.; Bowman, A.B. Huntington's disease associated resistance to Mn neurotoxicity is neurodevelopmental stage and neuronal lineage dependent. *Neurotoxicology* **2019**, *75*, 148–157. [CrossRef]
6. Rahman, M.M.; Dong, Z.; Naidu, R. Concentrations of arsenic and other elements in groundwater of Bangladesh and West Bengal, India: Potential cancer risk. *Chemosphere* **2015**, *139*, 54–64. [CrossRef]
7. USEPA. Drinking Water Health Advisory for Manganese. U.S. Environmental Protection Agency Office of Water, Washington, DC, EPA-822-R-04-003. pp. 1–49. 2004. Available online: https://www.epa.gov/sites/default/files/2014-09/documents/support_cc1_magnese_dwreport_0.pdf (accessed on 22 July 2025).
8. Kasaai, M.R. Use of Water Properties in Food Technology: A Global View. *Int. J. Food Prop.* **2014**, *17*, 1034–1054. [CrossRef]
9. Hoyland, V.W.; Knocke, W.R.; Falkinham, J.O.; Pruden, A.; Singh, G. Effect of drinking water treatment process parameters on biological removal of manganese from surface water. *Water Res.* **2014**, *66*, 31–39. [CrossRef]
10. Peng, C.-Y.; Korshin, G.V.; Valentine, R.L.; Hill, A.S.; Friedman, M.J.; Reiber, S.H. Characterization of elemental and structural composition of corrosion scales and deposits formed in drinking water distribution systems. *Water Res.* **2010**, *44*, 4570–4580. [CrossRef]
11. World Health Organization (WHO). *Guidelines for Drinking-Water Quality: Fourth Edition Incorporating the First Addendum*; WHO: Geneva, Switzerland, 2019.
12. Environment National Council (CONAMA), Resolução Nº 357, de 17 de Março de Dispõe Sobre a Classificação dos Corpos D'água e Diretrizes Ambientais Para o Seu Enquadramento, Bem Como Estabelece as Condições e Padrões de Lançamento De Efluentes, e da Outras Providências. 2005. Available online: https://conama.mma.gov.br/?option=com_sisconama&task=arquivo.download&id=450. (accessed on 20 August 2025).
13. Hermes, N.; Schneider, R.C.S.; Molin, D.D.; Riegel, G.Z.; Costa, A.B.; Corbellini, V.A.; Torres, J.O.M.; Malm, O. Environmental pathways and human exposure to manganese in southern Brazil. *An. Acad. Bras. Ciênc.* **2013**, *85*, 1275–1288. [CrossRef]
14. Melo, D.F.B.C.; Ribeiro, M.H.G.; Albuquerque Junior, E.C.; Gonçalves, E.A.P. Avaliação da Bacia do Rio Una-Pernambuco: Perspectiva da Qualidade da Água após a Construção de 4 Barragens para Contenção de Cheias. *Rev. Bras. Geogr. Fís.* **2018**, *11*, 612–627. [CrossRef]
15. Mollo, V.M.; Nomngongo, P.N.; Ramontja, J. Evaluation of Surface Water Quality Using Various Indices for Heavy Metals in Sasolburg. *Water* **2022**, *14*, 2375. [CrossRef]
16. Monjardin, C.E.; Power, C.; Senoro, D.B. Spatio-Temporal Assessment of Manganese Contamination concerning River Morphology: A Study of the Boac and Mogpog Rivers in Marinduque, Philippines. *Sustainability* **2023**, *15*, 8276. [CrossRef]
17. Agarin, C.J.M.; Mascareñas, D.R.; Nolos, R.; Chan, E.; Senoro, D.B. Transition Metals in Freshwater Crustaceans, Tilapia, and Inland Water: Hazardous to the Population of the Small Island Province. *Toxics* **2021**, *9*, 71. [CrossRef]
18. Pinisakul, A.; Kruatong, N.; Vinitnantharat, S.; Wilamas, P.; Neamchan, R.; Sukkhee, N.; Werner, D.; Sanghaisuk, S. Arsenic, Iron, and Manganese Adsorption in Single and Trinary Heavy Metal Solution Systems by Bamboo-Derived Biochars. *C* **2023**, *9*, 40. [CrossRef]
19. Zhang, Z.; Xiao, C.; Adeyeye, O.; Yang, W.; Liang, X. Source and Mobilization Mechanism of Iron, Manganese, and Arsenic in Groundwater of Shuangliao City, Northeast China. *Water* **2020**, *12*, 534. [CrossRef]
20. Anastopoulos, I.; Kyzas, G.Z. Progress in batch biosorption of heavy metals onto algae. *J. Mol. Liq.* **2015**, *209*, 77–86. [CrossRef]

21. Tounsadi, H.; Khalidi, A.; Abdennouri, M.; Barka, N. Biosorption potential of Diplotaxis harra and Glebionis coronaria L. biomasses for the removal of Cd(II) and Co(II) from aqueous solutions. *J. Environ. Chem. Eng.* **2015**, *3*, 822–830. [CrossRef]
22. Abdeen, Z.; Mohammad, S.G.; Mahmoud, M.S. Adsorption of Mn ion on polyvinyl alcohol/chitosan dry blending from aqueous solution. *Environ. Nanotechnol. Monit. Manag.* **2015**, *3*, 1–9. [CrossRef]
23. Alfarra, S.R.; Ali, E.N.; Yusoff, M.M. Removal of Heavy Metals by Natural Adsorbent. *Int. J. Bios.* **2014**, *4*, 130–139.
24. Vera, M.M.; Flores, M.; Vanegas, E.; Cruzata, C.; Juela, D. Removal of Mn from aqueous solution via biosorption technology for a drinking water treatment plant: From laboratory-scale tests to semi-industrial scale predictions. *Chem. Eng. Res. Des.* **2023**, *193*, 787–800. [CrossRef]
25. Pena-Guzman, C.; Otalvaro-Alvarez, A.; Jimenez-Ariza, T. Use of oilseed crops biomass for heavy metal treatment in water. *Oil Crop Sci.* **2024**, *9*, 177–186. [CrossRef]
26. Giraldo-Bareno, Y.Y.; Pinzón-García, A.D.; Sousa, D.V.M.; Bomfim Filho, L.F.O.; Lopes, D.H.A.; Cortés, N.S.; Morávia, M.C.S.A.; Sinisterra, R.D.; Orlando, R.M. Efficient and easily scaled-up biosorbent based on natural and chemically modified macauba (*Acrocomia aculeata*) to remove Al^{3+}, Mn^{2+} and Fe^{3+} from surface water contaminated with iron mining tailings. *Talanta* **2023**, *256*, 124273. [CrossRef] [PubMed]
27. Cardoso, A.P.; Valdiviezo-Gonzales, N.S.C.L.; Veneu, D.M.; Pino, A.H.; Torem, M.L. Comparative evaluation of lead and manganese removal from contaminated water using cocos nucifera shell powder in batch and continuous adsorption systems. *S. Afr. J. Chem. Eng.* **2025**, *53*, 483–494. [CrossRef]
28. Savitri, S.; Reguyal, F.; Sarmah, A.K. A feasibility study on production, characterisation and application of empty fruit bunch oil palm biochar for Mn2+ removal from aqueous solution. *Environ. Pollut.* **2023**, *318*, 120879. [CrossRef] [PubMed]
29. Dal-Bó, A.G.; Westrup, J.L.; Fiorin, D.G.; Ruschel, P.M.C.; da Silva, C.K.H.; Cercena, R.; Peterson, M.; Colonetti, E.; Fernandes, A.N. Efficient removal of Mn2+ ions from aqueous solutions using apple pomace biochar. *Chem. Eng. Commun.* **2024**, *211*, 84–101. [CrossRef]
30. Hussain, M.; Ali, A.S.; Kousar, T.; Mahmood, F.; Haruna, A.; Zango, Z.U.; Adamu, H.; Kotp, M.G.; Abdulganiyyu, I.A.; Keshta, B.E. Efficient removal of manganese (II) ions from aqueous solution using biosorbent derived from rice husk. *Discov. Sustain.* **2025**, *5*, 100047. [CrossRef]
31. Araújo, C.S.T.; Carvalho, D.C.; Rezende, H.C.; Almeida, I.L.S.; Coelho, L.M.; Coelho, N.M.M.; Marques, T.L.; Alves, V.N. Bioremediation of Waters Contaminated with Heavy Metals Using Moringa oleifera Seeds as Biosorbent. In *Applied Bioremediation—Active and Passive Approaches*; Patil, Y.B., Rao, P., Eds.; InTech: London, UK, 2013.
32. Nwagbara, V.U.; Iyama, W.A.; Chigayo, K.; Kwaambwa, H.M. Efficiency of *Moringa Oleifera* Seed Biomass in the Removal of Lead (II) Ion in Aqueous Solution. *Eur. J. Appl. Sci.* **2022**, *10*, 412–429.
33. Meneghel, A.P.; Gonçalves, A.C.; Rubio, F.; Dragunski, D.C.; Lindino, C.A.; Strey, L. Biosorption of cadmium from water using moringa (Moringa oleifera Lam.) Seeds. *Water Air Soil Pollut.* **2013**, *224*, 1383. [CrossRef]
34. Silva, M.O.; Camacho, F.P.; Ferreira-Pinto, L.; Giufrida, W.M.; Vieira, A.M.S.; Visentainer, J.V.; Vedoy, D.R.L.; Cardozo-Filho, L. Extraction and Phase Behaviour of *Moringa oleifera* Seed Oil Using Compressed Propane. *Can. J. Chem. Eng.* **2016**, *94*, 2195–2201. [CrossRef]
35. Carmo, S.N.; Sousa Neto, J.A.; Alves, V.N.; Coelho, L.M.; Coelho, N.M.M. Selective Extraction of Manganese using *Moringa oleifera* Seeds as Bioadsorbent. *Br. J. Anal. Chem.* **2019**, *6*, 27–37.
36. Wang, L.; Zhang, J.; Wang, A. Removal of methylene blue from aqueous solution using chitosan-g-poly(acrylic acid)/montmorillonite superadsorbent nanocomposite. *Colloids Surf. A Physicochem. Eng. Asp.* **2008**, *322*, 47–53. [CrossRef]
37. Zafar, M.N.; Aslam, I.; Nadeem, R.; Munir, S.; Rana, U.A.; Khan, S.U.-D. Characterization of chemically modified biosorbents from rice bran for biosorption of Ni(II). *J. Taiwan Inst. Chem. Eng.* **2015**, *46*, 82–88. [CrossRef]
38. Langmuir, I. The adsorption of gases on plane surfaces of glass, mica, and platinum. *J. Am. Chem. Soc.* **1918**, *40*, 1361–1403. [CrossRef]
39. Lalhruaitluanga, H.; Jayaram, K.; Prasad, M.N.V.; Kumar, K.K. Lead(II) adsorption from aqueous solutions by raw and activated charcoals of Melocanna baccifera Roxburgh (bamboo)-A comparative study. *J. Hazard. Mater.* **2010**, *175*, 311–318. [CrossRef]
40. Lagergren, S. Zur theorie der sogenannten adsorption gelster stoffe, Kungliga Svenska Vetenskapsakademiens. *Handlingar* **1898**, *24*, 1–39.
41. Ho, Y.S.; Mckay, G. The kinetics of sorption of basic dyes from aqueous solution by sphagnum moss peat. *Can. J. Chem. Eng.* **1998**, *76*, 822–827. [CrossRef]
42. Marques, T.L.; Alves, V.N.; Coelho, L.M.; Coelho, N.M.M. Removal of Ni(II) from aqueous solution using Moringa oleifera seeds as a bioadsorbent. *Water Sci. Technol.* **2012**, *65*, 1435–1440. [CrossRef] [PubMed]
43. Tavares, F.O.; Pinto, L.A.M.; Vicentini, J.C.M.; Vieira, M.F.; Bergamasco, R.; Vieira, A.M.S. Analysis of the influence of natural adsorbent functionalization (*Moringa oleifera*) for Pb(II) removal from contaminated water. *Environ. Prog. Sustain. Energy* **2020**, *39*, e13318. [CrossRef]

44. Kroon-Batenburg, L.M.J.; Kroon, J. The crystal and molecular structures of cellulose I and II. *Glycoconj. J.* **1997**, *14*, 677–690. [CrossRef]
45. Reddy, D.H.K.; Seshaiah, K.; Reddy, A.V.R.; Lee, S.M. Optimization of Cd(II), Cu(II) and Ni(II) biosorption by chemically modified Moringa oleifera leaves powder. *Carbohydr. Polym.* **2012**, *88*, 1077–1086. [CrossRef]
46. Alves, V.N.; Coelho, N.M.M. Selective extraction and preconcentration of chromium using Moringa oleifera husks as biosorbent and flame atomic absorption spectrometry. *Microchem. J.* **2013**, *109*, 16–22. [CrossRef]
47. Esfandiar, N.; Nasernejad, B.; Ebadi, T. Removal of Mn from groundwater by sugarcane bagasse and activated carbon (a comparative study): Application of response surface methodology (RSM). *J. Ind. Eng. Chem.* **2014**, *20*, 3726–3736. [CrossRef]
48. Kumar, D.; Gaur, J.P. Metal biosorption by two cyanobacterial mats in relation to pH, biomass concentration, pretreatment, and reuse. *Bioresour. Technol.* **2011**, *102*, 2529–2535. [CrossRef]
49. Basu, M.; Guha, A.K.; Ray, L. Biosorptive removal of lead by lentil husk. *J. Environ. Chem. Eng.* **2015**, *3*, 1088–1095. [CrossRef]
50. Kalavathy, H.; Miranda, M.L.R. Moringa oleifera-A solid phase extractant for the removal of copper, nickel and zinc from aqueous solutions. *Chem. Eng. J.* **2010**, *158*, 188–199. [CrossRef]
51. Fseha, Y.H.; Sizirici, B.; Yildiz, I. Manganese and nitrate removal from groundwater using date palm biochar: Application for drinking water. *Environ. Adv.* **2022**, *8*, 100237. [CrossRef]
52. Çifçi, D.I.; Meriç, S. Manganese adsorption by iron impregnated pumice composite. *Colloids Surf. A Physicochem. Eng. Asp.* **2017**, *522*, 279–286. [CrossRef]
53. Hayward, D.O.; Trapnell, B.M.W. *Chemisorption*, 2nd ed.; Butterworths: London, UK, 1964.
54. Viotti, P.V.; Moreira, W.M.; Santos, O.A.A.; Bergamasco, R.; Vieira, A.M.S.; Vieira, M.F. Diclofenac removal from water by adsorption on *Moringa oleifera* pods and activated carbon: Mechanism, kinetic and equilibrium study. *J. Clean. Prod.* **2019**, *219*, 809–817. [CrossRef]
55. Januário, E.F.D.; Vidovix, T.B.; Araújo, L.A.; Beltran, L.B.; Bergamasco, R.; Vieira, A.M.S. Investigation of *Citrus reticulata* peels as an efficient and low-cost adsorbent for the removal of safranin orange dye. *Environ. Technol.* **2022**, *43*, 4315–4329. [CrossRef]
56. Davis, T.A.; Mucci, A.; Volesky, B. A review of the biochemistry of heavy metal biosorption by brown algae. *Water Res.* **2003**, *37*, 4311–4330. [CrossRef] [PubMed]

Disclaimer/Publisher's Note: The statements, opinions and data contained in all publications are solely those of the individual author(s) and contributor(s) and not of MDPI and/or the editor(s). MDPI and/or the editor(s) disclaim responsibility for any injury to people or property resulting from any ideas, methods, instructions or products referred to in the content.